

## In Situ Underfilm Corrosion Rate Measurements by Magnetic and Electrochemical Techniques

N. J. Cantini,<sup>a</sup> D. B. Mitton,<sup>a</sup> N. Eliaz,<sup>a,\*</sup> G. Leisk,<sup>a</sup> S. L. Wallace,<sup>a</sup> F. Bellucci,<sup>b,\*\*</sup>  
G. E. Thompson,<sup>c,\*\*\*</sup> and R. M. Latanision<sup>a,\*\*</sup>

<sup>a</sup>H. H. Uhlig Corrosion Laboratory, Massachusetts Institute of Technology, Cambridge, Massachusetts 02139, USA.

<sup>b</sup>Department of Materials and Production Engineering, University of Naples Federico II, Naples 80125, Italy.

<sup>c</sup>Corrosion and Protection Centre, University of Manchester Institute of Science and Technology, Manchester M60 1QD, United Kingdom

A novel magnetic approach is introduced to measure the corrosion rate of bare and coated ferromagnetic materials. The corrosion of bare and acrylic-coated cobalt is monitored *in situ* and in real-time by coupling electrochemical impedance spectroscopy (EIS) and saturation magnetic moment measurements using a vibrating sample magnetometer (VSM). For the first time, the corrosion rate beneath a polymer coating is measured accurately *in situ*; additionally, it is suggested that the VSM can be used to enhance the interpretation of EIS data.

© 2000 The Electrochemical Society. S1099-0062(00)02-019-8. All rights reserved.

Manuscript submitted February 3, 2000; revised manuscript received March 10, 2000. Available electronically April 13, 2000.

Organic coatings are often used to delay the onset and reduce the rate of corrosion.<sup>1</sup> However, such coatings are not impervious to aqueous solutions, which might ultimately lead to the insidious phenomenon of underfilm corrosion.<sup>1,2</sup> Underfilm corrosion cannot be monitored by direct weight loss measurements because of water absorption in the coating, trapping of corrosion products beneath the coating, and the nonuniform character of the degradation.<sup>3</sup>

Electrochemical impedance spectroscopy (EIS) has been widely used to study corrosion protection by organic coatings. Advantages of this technique over dc and conventional techniques include the absence of any significant perturbation to the system, its applicability to the assessment of low-conductivity media such as polymers, and the existence of a frequency component that may provide mechanistic information.<sup>1,4</sup> EIS, however, has some significant drawbacks. At low frequencies, where underfilm corrosion reactions are probed, experimental difficulties and time constraints can complicate precise determination of the charge-transfer resistance ( $R_{ct}$ ) and the double-layer capacitance ( $C_{dl}$ );<sup>5</sup> additionally, the Warburg impedance may exhibit a masking effect,<sup>6,7</sup> and inductive loops or new time constants are sometimes observed.<sup>8</sup> Further, due to the long measurement time required, both the corrosion rate and corrosion potential can change during the experiment. There has also been no evidence that  $R_{ct}$  can be equated to the polarization resistance ( $R_p$ ) and used in the Stern-Geary equation to calculate the underfilm corrosion rate.<sup>9</sup> Finally, in-depth mechanistic and kinetic information on the corroding interface can easily be overlooked in EIS by modeling the system with an oversimplified equivalent circuit.<sup>4</sup>

Magnetic measurements may also be used to monitor corrosion. The saturation magnetic moment ( $\mu_s$ ) of a ferromagnetic material is proportional to the mass (volume) of the material. Since the signal from a ferromagnetic substrate is much larger than the signals of either a polymer coating or nonferromagnetic corrosion products, decreases in  $\mu_s$  can be measured and used to assess the mass loss due to corrosion.<sup>10,11</sup>

The vibrating sample magnetometer (VSM), invented by Foner of MIT,<sup>12</sup> has been used since the late 1950s to investigate the magnetic properties of materials.<sup>13</sup> Its operating principle involves the detection of a dipole field from a magnetic sample when it is vibrated perpendicularly to a uniform magnetizing field.<sup>14</sup> Since changes of magnetic moment as small as  $10^{-5}$  emu can be detected,<sup>14</sup> this

technique can monitor very low mass losses (typically  $<100 \mu\text{g}$ ). In addition to being nondestructive and permitting convenient measurements using commercial electromagnets, this technique is highly accurate.

The objective of this work is twofold: to verify the applicability of the VSM for measuring the corrosion rate of bare and coated ferromagnetic materials, and to suggest a way of using it to enhance the interpretation of EIS data.

### Experimental

Cobalt was chosen for this work since it is ferromagnetic and corrodes to produce nonferromagnetic oxides.<sup>15</sup> Sample size was an important consideration in this research. On the one hand, since small amounts of corrosion were expected (given the presence of a coating and short exposure times), the initial volume of the cobalt had to be sufficiently small to ensure significant change in saturation magnetic moment; *i.e.*, larger than the sensitivity of the VSM ( $\pm 0.25\%$ ). In addition, the sample had to be placed within a reduced VSM pole gap (to achieve increased magnetic fields) and satisfy the magnetic dipole approximation.<sup>16</sup> On the other hand, sample size needed to be large enough to avoid ohmic errors during electrochemical tests,<sup>17</sup> and to provide a sufficiently large exposed area for the electrochemical measurements to be meaningful.

To prepare the samples, silicon wafers were electron-beam deposited with a 3200 Å thick pure cobalt layer (thickness measured by profilometry). The wafers were then sectioned into rectangular samples of approximately 0.7 × 2.3 cm. Selected samples were coated with a transparent acrylic varnish. The polymer was undercured to make it more permeable to moisture and ions by decreasing the degree of cross-linking. Masking was used to prevent localized corrosion phenomena. VSM and EIS tests were performed *in situ* and in real-time on the cobalt samples using a novel miniature cell design.<sup>18</sup> This cell design satisfied the previous sample dimension requirements and used weakly diamagnetic and paramagnetic materials. The cell was filled with a 0.5 M NaCl (pH 7) solution, refreshed daily from a reservoir to which purified air was continuously bubbled. For EIS measurements, a modified three-electrode setup was used, in which a Ag/AgCl miniature reference electrode was immersed directly in the cell. A Schlumberger Solartron 1286 electrochemical interface and a Solartron 1250 impedance/gain-phase analyzer, connected to a PC by an IEEE/GPIB interface, were used. EISTEST, a software package developed at the H. H. Uhlig Corrosion Laboratory, was used to control the sweeps. The open-circuit potential (OCP) was monitored for more than 20 min before each sweep. Frequency ranges of 10 kHz to 10 mHz and 65 kHz to

\* Electrochemical Society Student Member.

\*\* Electrochemical Society Active Member.

\*\*\* Electrochemical Society Fellow.

<sup>z</sup> E-mail: neliaz@mit.edu

5 mHz were selected for the uncoated and polymer-coated samples, respectively. The amplitudes of the superimposed potential were 5 and 20 mV for the uncoated and coated samples, respectively. EIS data was analyzed with ZView software (Scribner Associates). Potentiodynamic measurements were carried out with a traditional three-electrode setup and a saturated calomel electrode (SCE) to estimate the Tafel slopes for bare cobalt.

Corrosion rates were obtained from electrochemical measurements, using the expression

$$r = (a i_{\text{corr}}) / nF \quad [1]$$

where  $a$  is the atomic mass of the corroded metal (58.933 g/mol),  $n$  the number of electrons transferred in the reaction (2 equiv/mol),  $F$  is Faraday's constant (96,487 C/equiv), and  $i_{\text{corr}}$  the corrosion current density. Substituting the Stern-Geary relation for  $i_{\text{corr}}$ , the following equation is obtained

$$r = (a/nFA R_p) [\beta_a |\beta_c| / 2.3(\beta_a + |\beta_c|)] \quad [2]$$

where  $A$  is the exposed surface area,  $R_p$  the polarization resistance, and  $\beta_a$  and  $\beta_c$  the anodic and cathodic Tafel slopes, respectively. A series of potentiodynamic measurements yielded  $\beta_a = 81$  mV, and  $|\beta_c| = 367$  mV. The cumulative mass loss was subsequently obtained by integrating the normalized time-dependent corrosion rate on time

$$\Delta m = \int_{t_0}^{t_n} r A dt \quad [3]$$

Magnetic measurements were carried out at room temperature with a model 880 VSM from Digital Measurement Systems, Inc. First, calibration was carried out using a standard high-purity nickel disk. Second, the reference electrode was removed from the miniature cell, and the cell was completely filled with solution, sealed, and mounted tightly onto a cantilever. Third, the magnetic moment of each cell was recorded six times in the range 8,050-10,000 Oe. The total magnetic moment,  $\mu$ (H), included contributions from the ferromagnetic cobalt and from all of the remaining paramagnetic and diamagnetic materials present in the cell. Fortunately, the magnetic moment of a ferromagnetic material is independent of the applied field above its saturation field. Therefore, the  $\mu_s$  of cobalt could be separated readily from the contributions of the paramagnetic and diamagnetic materials by linear regression. Corrections for sample size (described in Ref. 16) were applied to the calculated values of  $\mu_s$ .

Assuming that the value of the saturation magnetization (the maximal magnetic moment density),  $M_s$ , is not affected by corrosion phenomena, the mass loss due to corrosion was calculated by

$$\Delta m = ((\mu_{s,0} - \mu_{s,f}) / \mu_{s,0}) m_0 \quad [4]$$

where  $m_0 = (\mu_{s,0} / M_{s,b}) \rho$  is the initial mass of cobalt,  $\mu_{s,0}$  is the saturation moment before exposure to the electrolyte,  $\mu_{s,f}$  is the saturation moment after a certain exposure time,  $M_{s,b}$  is the bulk cobalt saturation magnetization (1400 emu/cm<sup>3</sup>),<sup>19</sup> and  $\rho$  the density of cobalt (8.832 g/cm<sup>3</sup>). Corrosion rates were calculated by plotting the cumulative mass loss vs. time, performing polynomial fitting, differentiating the fitting expressions over time, and normalizing to the exposed area.

To compare between mass loss values obtained from VSM and gravimetric measurements, rectangular samples (approximately 1.5 x 1.2 cm) were cut from pure cobalt foils (0.25 mm thick). Corrosion was induced under potentiostatic conditions in an acidified solution using a conventional three-electrode setup.

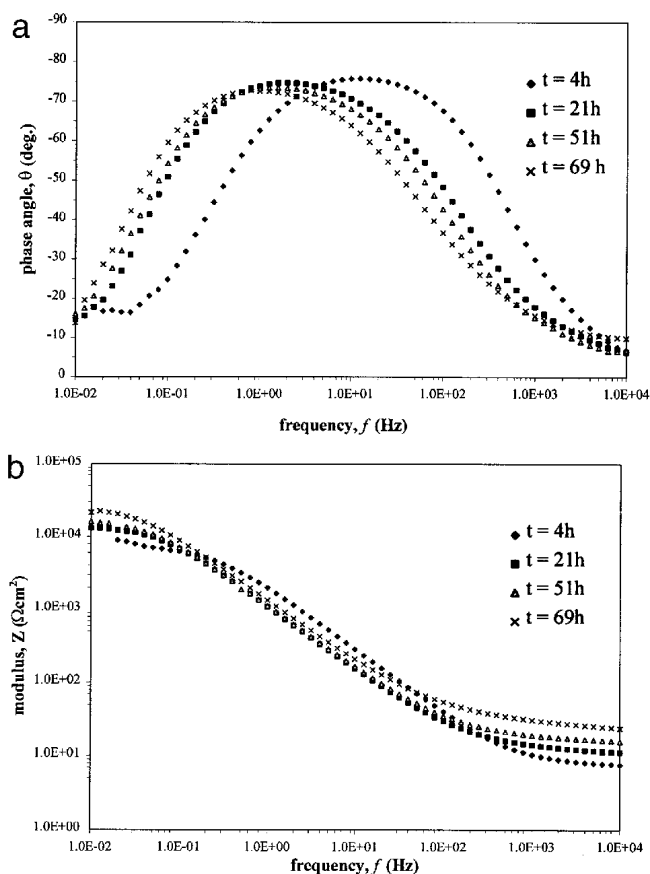


Figure 1. EIS Bode plots for bare cobalt after (a) 4, (b) 21, (c) 51, and (d) 69 h of immersion.

## Results and Discussion

**Bare samples.**—Figure 1 presents the EIS Bode plots for the uncoated cobalt metal with increasing times of exposure to the electrolyte. The charge-transfer resistance, or polarization resistance, was measured as the difference between the two plateaus in the modulus plots. Similar values were obtained by measuring the real axis chord of the depressed semicircle in the Nyquist plot. Sweeps performed at times longer than 69 h of immersion yielded spectra, which could not be deconvolved for analysis. Such behavior may result from the significantly reduced volume of cobalt and the exposure of the silicon wafer. Visually, large greenish and brownish spots were observed on the surface after only a few hours, suggesting the formation of  $\text{Co}(\text{OH})_2$ .<sup>20</sup>

Figure 2a shows the relative change in the saturation magnetic moment vs. the relative change in mass for the cobalt foil samples, as obtained from VSM and gravimetric measurements, respectively.<sup>10</sup> Excellent correlation is evident, supporting the applicability of the VSM for mass loss measurements. Excellent correlation between the cumulative mass loss values measured by EIS and VSM is also evident for uncoated silicon/cobalt wafers (Fig. 2b). These results support the validity of determining  $R_{ct}$  (or  $R_p$ ) directly from the Bode plot under such conditions. It is also evident from Fig. 2b that the corrosion rate (proportional to the slope of the curve) decreases with time. This behavior is typical for corrosion of bare metals.<sup>21</sup> Finally, the curve exhibits asymptotic behavior, which indicates that all of the initial mass of cobalt in the exposed area ( $\sim 170$   $\mu\text{g}$ ) was consumed by corrosion after immersion for about 120 h.

**Coated samples.**—In polymer-coated samples, EIS analysis could only be made after some immersion time, when the cobalt beneath the

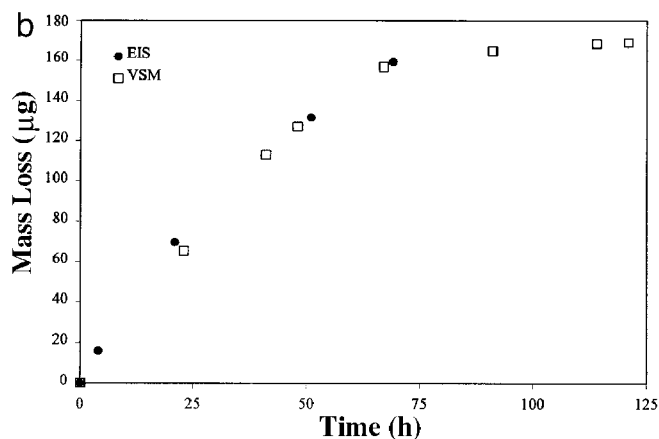
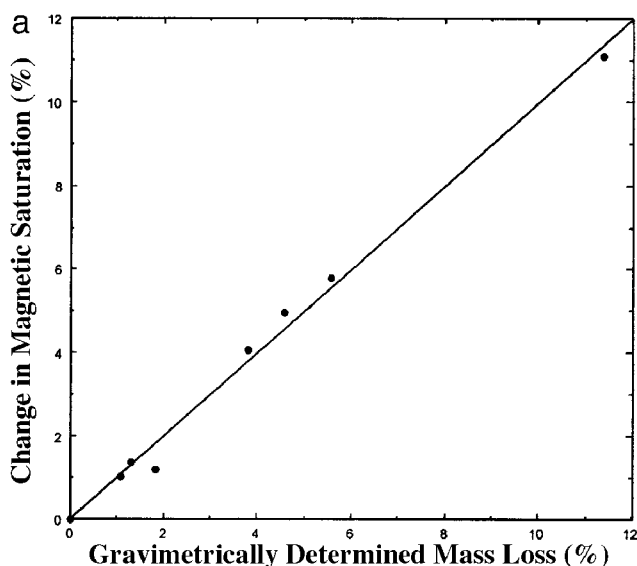


Figure 2. (a) The relative change in saturation magnetic moment (VSM) vs. relative change in mass (gravimetric measurements) for bare cobalt (b) cumulative mass loss of bare cobalt, as obtained from EIS and VSM measurements.

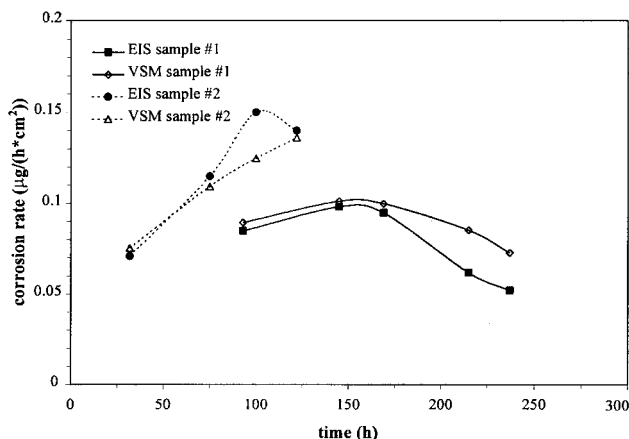
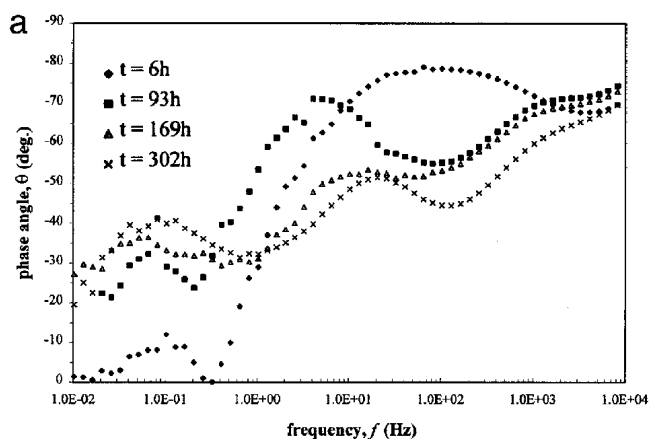


Figure 4. Underfilm corrosion rates of polymer-coated cobalt samples, as obtained from EIS and VSM measurements.

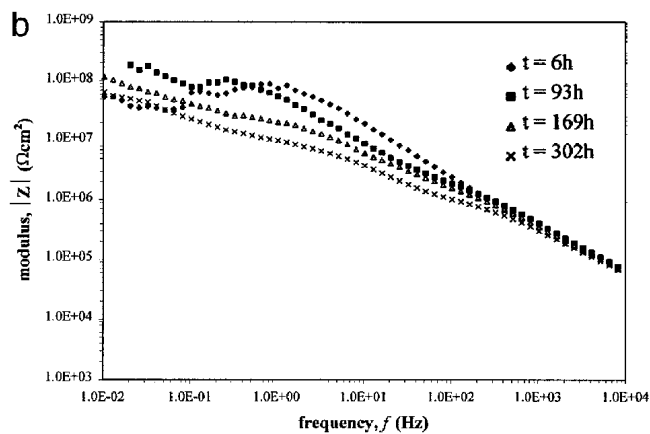


Figure 3. EIS Bode plots for acrylic-coated cobalt (sample no. 1) after (a) 6, (b) 93, (c) 169, and (d) 302 h of immersion. Only plots b and c may be used for the determination of  $R_{ct}$ .

polymer was clearly exposed. EIS analysis was also not possible after long immersion times, likely due to masking effects of diffusion through corrosion products which had formed at the bottom of defects in the coating, and/or exposure of the silicon substrate. Selected Bode plots for the coated samples are shown in Fig. 3.

Figure 4 reveals the underfilm corrosion rates of polymer-coated cobalt samples, as obtained by both EIS and VSM measurements. The corrosion rates increase with time, reach peak values, and subsequently decrease, as is typical for coated samples.<sup>21</sup> Moreover, lower mass losses were observed for the coated samples in comparison with the uncoated samples, as anticipated. Visual and microscopic observations indicated that corrosion initiated at defects, and usually progressed in a branchlike fashion. The slightly different corrosion rates observed for the two coated samples likely resulted from differences in the distribution of defects in the acrylic coating. Good agreement between the corrosion rate values obtained from EIS and VSM measurements is apparent in Fig. 4. Discrepancies in data between the two techniques may result from changes in the Tafel parameters with time and inaccurate determination of  $R_{ct}$  from the Bode and Nyquist plots. The

good agreement between EIS and VSM results supports, for the first time, the validity of using  $R_{ct}$  and the Stern-Geary relation (Eq. 2) for underfilm corrosion rate evaluation. However, as shown here, such an evaluation can be made on the basis of EIS only well after corrosion initiates, and when diffusion (or other) processes do not mask the appearance of the substrate in the EIS spectra. Experimental approaches that can overcome masking effects are currently under investigation. In addition, efforts to deconvolve the EIS spectra and to better define equivalent circuits with the aid of VSM results are in progress. For example, one may use the VSM to enhance the interpretation of EIS data through the following procedure: (i) measure the mass loss by means of a VSM; (ii) use this mass loss value to determine  $R_p$  (Eq. 2); (iii) examine the EIS spectra carefully and isolate the feature that most likely corresponds to the predetermined  $R_p$ .

### Conclusions

Based on *in situ* measurements of underfilm corrosion rate in acrylic-coated cobalt samples using electrochemical and magnetic techniques, the following conclusions are drawn.

1. Measurements of the saturation magnetic moment allow accurate *in situ* monitoring of corrosion rates of bare and polymer-coated ferromagnetic metals in the absence of ferromagnetic corrosion products.

2. Magnetic measurements may be used to improve the interpretation of EIS data, especially in the case of underfilm corrosion.

3. When the charge-transfer resistance can be determined unambiguously from EIS data, underfilm corrosion rates can be measured. The Stern-Geary relation may be used in these calculations.

### Acknowledgments

This work is partially supported by the National Science Foundation (NSF) through grant no. DMR-9708148.

The Massachusetts Institute of Technology assisted in meeting the publication costs of this article.

### References

1. D. A. Jones, *Principles and Prevention of Corrosion*, p. 475, Macmillan Publishing Company, New York (1992).
2. E. L. Koehler, in *Corrosion Control by Organic Coatings*, H. Leidheiser, Editor, p. 87, NACE, Houston, TX (1981).
3. W. J. Lorenz and F. Mansfeld, *Corros. Sci.*, **21**, 647 (1981).
4. *Impedance Spectroscopy-Emphasizing Solid Materials and Systems*, J. R. Macdonald, Editor, Wiley, New York (1987).
5. F. Mansfeld, S. L. Jeanjaquet, and M. W. Kendig, *Corros. Sci.*, **26**, 735 (1986).
6. P. Bonora, F. Deflorian, and L. Fedrizzi, *Electrochim. Acta*, **41**, 1074 (1996).
7. J. Dawson and D. John, *J. Electroanal. Chem.*, **110**, 37 (1980).
8. G. W. Walter, *Corros. Sci.*, **26**, 681 (1986).
9. F. Mansfeld, *Corrosion*, **36**, 301 (1981).
10. S. L. Wallace, M.S. Thesis, Massachusetts Institute of Technology, Cambridge (1999).
11. D. B. Mitton, Ph.D. Thesis, University of Manchester Institute of Science and Technology, Manchester, U.K. (1989).
12. S. Foner, *Rev. Sci. Instrum.*, **27**, 548 (1956).
13. K. D. McKinstry, C. E. Patton, C. A. Edmondson, P. J. McClure, and S. Kern, *Rev. Sci. Instrum.*, **62**, 779 (1991).
14. S. Foner, *Rev. Sci. Instrum.*, **30**, 548 (1959).
15. W. Betteridge, *Cobalt and Its Alloys*, Ellis Horwood Limited, England (1982).
16. A. Zieba and S. Foner, *Rev. Sci. Instrum.*, **53**, 1344 (1982).
17. A. Kuhn and J. Wellwood, *Br. Corros. J.*, **21**, 228 (1986).
18. D. B. Mitton, N. Eliaz, S. L. Wallace, N. J. Cantini, G. Leisk, F. Bellucci, G. E. Thompson, and R. M. Latanision, *J. Electrochem. Soc.*, To be submitted.
19. C. Kittel, *Introduction to Solid State Physics*, 7th ed., p. 449, John Wiley & Sons, New York (1996).
20. J. E. Thompson, *The Magnetic Properties of Materials*, p. 121, Newness Books, U.K. (1968).
21. L. M. Callow and J. D. Scantlebury, *J. Oil Colour Chem. Assoc.*, **64**, 119 (1981).